THESIS FOR THE DEGREE OF LICENTIATE OF ENGINEERING

Deactivation of SCR catalysts
Impact of sulfur and the use of biofuels

JOHANNA ENGLUND

CHALMERS

Department of Chemistry and Chemical Engineering
Division of Applied Surface Chemistry
Competence Centre of Catalysis
CHALMERS UNIVERSITY OF TECHNOLOGY
Gothenburg, Sweden 2018

Deactivation of SCR catalysts
Impact of sulfur and the use of biofuels
JOHANNA ENGLUND

Licentiatuppsatser vid Institutionen för kemi och kemiteknik
Chalmers tekniska högskola
Nr 2018-08

Department of Applied Chemistry
Competence Centre for Catalysis
Chalmers University of Technology
SE-412 96 Gothenburg
Telephone +46 31 772 1000

Typeset in LaTeX
Printed by Chalmers Reproservice
Gothenburg, Sweden 2018

Deactivation of SCR catalysts - Impact of sulfur and the use of biofuels

JOHANNA ENGLUND
Department of Chemistry and Chemical Engineering
Chalmers University of Technology

Abstract

In a near future, limits on CO_2 emissions from vehicles will be introduced, which requires development of more fuel-efficient engines and most likely a transition towards the use of more biofuels. With the implementation of biofuels several issues could arise, one being the lack of fuel standards for these new type of fuels, leading to higher concentrations of catalyst poisons compared to conventional fossil fuels. This work specifically focuses on catalyst poisoning originating from biofuels and is based on two papers.

The aim of the work presented in paper I is to study the influence of SO_2 on the low-temperature performance of a Cu-SSZ-13 SCR (selective catalytic reduction) catalyst. In particular the sulfur exposure temperature and the influence of the NO_2/NO_x ratio are considered, and two different regeneration temperatures are investigated. The results show that the temperature at which the Cu-SSZ-13 catalyst is exposed to SO_2 is a critical parameter. The lowest exposure temperature (220°C) resulted in the most pronounced deactivation, while the highest exposure temperature (400°C) caused the lowest degree of deactivation of the catalyst. It was also shown that the exposure to SO_2 resulted in decreased N_2O selectivity. Engine-aging of the Cu-SSZ-13 catalyst resulted in decreased SCR activity and increased selectivity towards N_2O formation, which most likely is caused by impurities from the fuel and engine-oil.
In paper II, the influence of the fuel on the functionality of a commercial vanadia-based SCR catalyst after extended field-operation is investigated. The NH_3-SCR activity, NH_3-oxidation activity, NH_3 adsorption capacity, specific surface area and surface composition were measured before and after field-operation in two heavy-duty Euro V vehicles fuelled with fatty acid methyl ester (FAME) and hydrotreated vegetable oil (HVO), respectively. For the catalyst samples taken from the vehicle fuelled with FAME, the NH_3-SCR activity, NH_3-oxidation activity and NH_3 adsorption capacity were significantly lower compared to the fresh sample and the samples taken from the vehicle fuelled with HVO. This is likely due to accumulation of catalyst poisons that originates from the FAME fuel that cause blocking of the active sites on the vanadia-based catalyst.

The studies of single poison compounds in lab-scale experiments are important for the understanding of catalyst deactivation mechanisms, however, there are many more parameters that dictates the deactivation in a vehicle. This can be seen from the engine-aged samples in both paper I and II where a single poison cannot fully explain the observed deactivation.

Keywords: Emission control; Biofuel; HVO; FAME; Sulfur; NO_x reduction; DeNOx; Catalyst deactivation; NH_3-SCR; Vanadia; Cu-SSZ-13; Cu-CHA; Activity test

List of Publications

This thesis is based on the following appended papers:

I. Chemical aging of Cu-SSZ-13 SCR catalysts for heavy-duty vehicles – Influence of sulfur dioxide
Sandra Dahlin, Cornelia Lantto, Johanna Englund, Björn Westerberg, Francesco Regali, Magnus Skoglundh and Lars J. Pettersson
Accepted, Catalysis Today, (2018), doi: 10.1016/j.cattod.2018.01.035

II. Post-mortem analysis of deNOx catalysts from biofueled heavy-duty vehicles
Johanna Englund, Sara Brazée, Jonas Jansson, Natalia M. Martin, Magnus Skoglundh and Per-Anders Carlsson
In manuscript

My Contributions to the Publications

Paper I
I participated in the planning of the SO_2 oxidation experiments and performed those experiments, interpreted the results together with my co-authors, and co-authored the manuscript.

Paper II
I supervised Sara Brazée and performed the flow reactor experiments and the data analysis of those experiments in collaboration with her, interpreted the results with my co-authors, and wrote the first draft of the manuscript.

Contents

Chapter 1

Introduction

Today we live in a society where our collective footprint on the planet earth far exceeds what is sustainable. One sector that contributes to the pollution of the atmosphere and biosphere is transportation. We all depend on transportation of humans and goods not least to satisfy food and materialistic needs. Due to this dependency on transportation legislation was introduced to try to control the amount of emissions coming from this sector.

The emission standards for heavy-duty vehicles that are valid in Europe at the present time are the Euro VI standards, limiting the emissions of nitrogen oxides (NO_x) and particulate matter (PM) to 0.40 and 0.01 g/kWh, respectively. These limits must be met during the lifetime of the vehicle which is 7 years or 700,000 km whichever is fulfilled first [1]. To reduce the impact from the transportation sector, the emission standards are becoming more and more stringent. Soon there will also be standards on carbon dioxide (CO_2) emissions, which will lead to more efficient engines hence to lower exhaust temperatures and/or higher outlet NO_x emissions from the engine [2, 3]. Both colder emissions and higher engine out concentrations of NO_x lead to higher demands on activity and selectivity of the catalysts in the aftertreatment system. Aftertreatment systems for heavy-duty vehicles consist of several parts, two being the oxidation catalyst and the selective catalytic reduction (SCR) catalyst [4]. The function of the oxidation catalyst is to oxidize carbon monoxide (CO) and hydrocarbons (HC) into CO_2 and water since both CO and HC are compounds that are harmful for health and environment. It is not just the CO and HC that needs to be removed from the exhausts, PM is trapped by the particulate filter and NO_x is reduced to nitrogen and water in the SCR catalyst. The leading technology for NO_x reduction is ammonia (NH_3)

SCR where the NH_3 is derived from urea and used as the reducing agent for NO_x over the SCR catalyst. Ammonia itself is a potent greenhouse gas so slip of this compound needs to be minimized as well.

The state-of-the-art catalyst for NH_3-SCR applications used today is based on small-pore zeolites, functionalized with copper, although vanadia-based catalysts are also used. The zeolites have high activity and selectivity towards NH_3-SCR and they are also thermally stable. However they are sensitive to sulfur poisoning. Moving towards increased use of renewable fuels like biodiesel, sulfur will be increasingly present in the exhausts. Further, studies should be performed on how to regenerate these materials after deactivation as well as determine deactivation mechanisms to achieve a better understanding of the poisoning phenomena. The vanadia-based catalysts are resistant to sulfur poisoning but susceptible to poisoning from other compounds containing alkali metals, which are present in e.g. biofuels [5–12]. Many studies of deactivation of catalysts have been conducted in small lab-scale experiments with single elements but data from real-driving is lacking. To grasp the full impact on the catalysts when using alternative fuels such data is useful [13–15].

1.1 Objectives

There are two main objectives of this study. The first is to study the effect of SO_2 on the low-temperature activity of a Cu-SSZ-13 SCR catalyst. The effect of the SO_2 exposure temperature and the influence of the NO_2/NO_x ratio on the activity of the catalyst are investigated. In addition, two different regeneration temperatures are compared and engine-aged samples are tested and compared with lab-aged samples as well. The second objective is to compare the impact of two different biofuels, HVO (hydrotreated vegetable oil) and FAME (fatty acid methyl ester), on the catalytic performance of a commercially available vanadia-based SCR catalyst used in Euro V heavy-duty vehicles before and after operation in the field. The NH_3-SCR activity, NH_3-oxidation activity, NH_3 adsorption capacity, specific surface area and surface composition of the vanadia-based catalyst are measured before and after field-operation.

Chapter 2

Background

Deactivation of automotive catalysts is a well studied phenomenon, however new catalysts and new types of fuels are continuously introduced on the market, which causes new problems with catalyst deactivation. When new emission standards are introduced that limits the amount of CO_2 that is allowed to be emitted from the vehicle, biofuels will be an attractive alternative to fossil fuels. When combusted in the engine, these fuels do not necessarily emit less CO_2 from the vehicle, however as the source of the carbon is non-fossil, the net CO_2 emissions to the atmosphere are much lower compared to fossil fuels.
The following section will introduce two types of catalysts used for removing NO_x from engine exhausts and the most important mechanisms of deactivation of these catalysts will be described.

2.1 NH_3-SCR application

NO_x in the exhausts from petrol powered vehicles, operating with stoichiometric combustion, is effectively removed by the so-called tree-way catalyst. However, this catalyst has a narrow operating window when it comes to the air/fuel ratio. The diesel engine operates at oxygen excess, which means that the tree-way catalyst is incapable of NO_x reduction for this application. To reduce the NO_x present in emissions from heavy-duty vehicle engines to nitrogen (N_2) and water (H_2O), a SCR catalyst in combination with a reducing agent is used instead of the tree-way catalyst. The most commonly used reducing agent is ammonia that is injected into the flue gas as urea [16]. Urea is thermally decomposed and hydrolyzed into ammonia and CO_2 at the elevated temperature

in the flue gas. The SCR reaction can occur in several ways depending on the NO_2/NO_x ratio. The most common route called standard SCR follows the path of equation 2.1. This is the route the reaction follows when the levels of NO_2 in the gas stream are low [17].

$$4NO + 4NH_3 + O_2 \rightarrow 4N_2 + 6H_2O \tag{2.1}$$

The oxidation catalyst placed up stream of the SCR catalyst can oxidize NO to NO_2 and when the ratio of NO_2/NO_x reaches 0.5 the so called fast-SCR reaction takes place according to reaction 2.2 [18, 19].

$$2NO + 4NH_3 + 2NO_2 \rightarrow 4N_2 + 6H_2O \tag{2.2}$$

As mentioned the SCR reaction takes place over a catalyst. The most commonly used catalysts for this purpose in heavy-duty vehicles are the vanadia-based catalyst and the copper-exchanged chabazite, SSZ-13, catalyst shown in Figure 2.1.

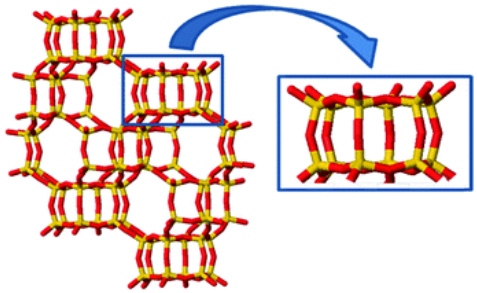

Figure 2.1: Chabazite structure [20].

2.1.1 The Cu-SSZ-13 catalyst

When the need for more durable and selective SCR catalysts increased zeolite-based systems attracted interest. Zeolites are porous materials built by aluminum, silicon and oxygen atoms in different ratios. The first zeolite that was investigated for the NH_3-SCR application was the copper-exchanged ZSM-5 zeolite [21–23]. Brandenberger et al. explain how the Si/Al ratio and cage size of the ZSM-5 makes it a better candidate for NH_3-SCR than other existing zeolites at the time. Their study also shows that copper-exchanged zeolite beta is active for NH_3-SCR [23].

In 2009 a new zeolite was patented [24]. This was the copper exchanged SSZ-13 zeolite (Cu-SSZ-13) used widely today due to the superior activity and stability it shows

for the NH_3-SCR reaction in comparison with other zeolites [25]. The synthetic zeolite SSZ-13 has the same structure (CHA) as the naturally ocurring zeolite chabazite with small eight-membered ring pores (3.8 Å) [26]. The copper-exchanged zeolite SSZ-13 shows high thermal stability and it is suggested that the high stability comes from the location of the copper ions within the cages of the zeolite [27].

2.1.2 The vanadia-based catalyst

The traditional catalyst used for NH_3-SCR is the vanadia-based catalyst where vanadium pentoxide (V_2O_5) is supported on the anatase structure of titanium dioxide (TiO_2) [28]. Vanadia catalysts contain between 1.0 and 2.5 wt.% of V_2O_5 and the catalyst is promoted by tungsten trioxide (WO_3). The WO_3 increases the activity of the catalyst and widens the temperature range where it is active. It also helps to prevent poisoning by alkali metals and sulfur dioxide (SO_2) [29]. Even with the promoter present in the catalyst the thermal stability is not as high as for the Cu-SSZ-13 catalyst. At higher temperatures, above 670°C, V_2O_5 may form volatile compounds that are toxic for humans so the operation temperature needs to be kept below this limit [7].

2.2 Catalyst deactivation

A catalyzed reaction does not consume the catalyst which means that in theory a catalyst could be used for eternity however in practice, this is not the case due to deactivation of the catalyst with time of operation. Catalyst deactivation can proceed via different deactivation mechanisms that are summarized in Figure 2.2. The mechanisms are described by Bartholomew and represented by the routes (a) thermal degradation (b) poisoning (c) fouling and (d) vapour compound formation where the active phase forms volatile compounds that leave the surface leading to loss of active phase [30].

Thermal degradation leads to loss of active phase in several aspects. The one illustrated in Figure 2.2a is crystallite growth of the active phase, which also is called sintering. This phenomenon primarily occur at temperatures above 500°C and the presence of water enhances the sintering rate [30]. Additional deactivation caused by thermal degradation comes from pore collapse and/or chemical transformation of the catalytically active phase to non-active phases. The loss of active phase due to thermal degradation is irreversible.

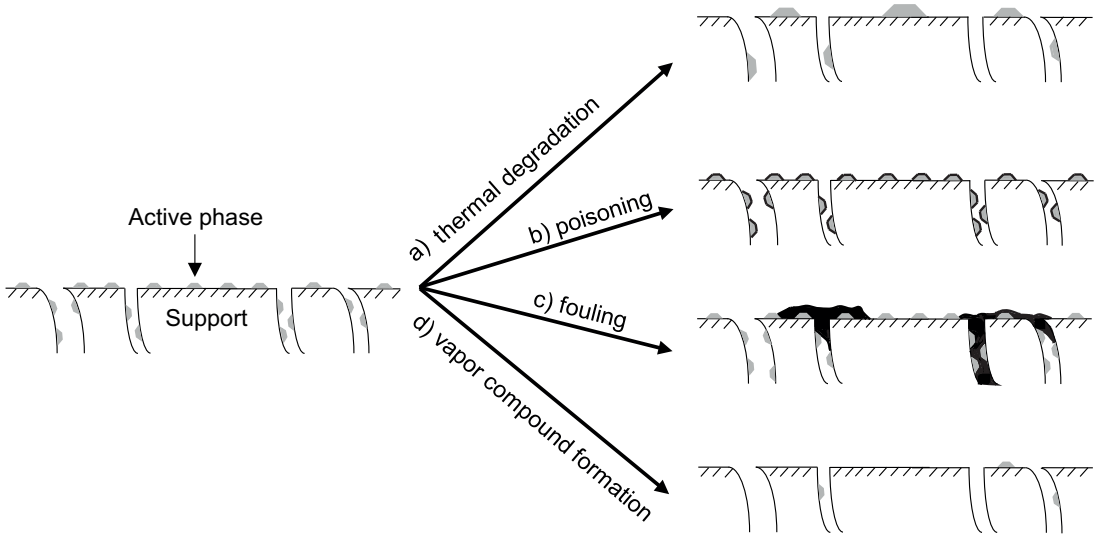

Figure 2.2: Deactivation mechanisms for a supported catalyst [31].

A second route of deactivation is catalyst poisoning represented by the black layer covering the active sites in Figure 2.2b. Poisoning is caused by compounds that interact with the active sites in a way that hinders reaction from taking place over those sites. Catalyst poisoning can be weak or strong depending on how strongly the compound (catalyst poison) interacts with the active sites of the catalyst. Fouling, shown in Figure 2.2c is caused by physical deposition of compounds, often carbon based, onto the surface of the catalyst which hinders adsorption of reactants on the active sites due to blocking of pores and/or active sites. Under certain conditions the active phase can form volatile compounds and leave the surface, this is called vapour compound formation. Some of the volatile compounds formed this way can be toxic, one example being volatile vanadium compounds formed from vanadium SCR catalysts at high temperatures [7].

2.2.1 Sulfur

A common type of deactivation when it comes to catalysts used for vehicle emission control is poisoning by sulfur containing compounds. This is due to the fact that both diesel and petrol contain sulfur. The influence of sulfur, like all catalyst poisons, on the catalytic properties of the catalyst depends on the nature of the active sites. This means that whenever a new type of catalyst is introduced, sulfur deactivation studies need to be performed.

The vanadia-based SCR catalyst show high resistance towards sulfur poisoning. However, the newer Cu-SSZ-13 SCR catalyst is more susceptible to sulfur poisoning [32,33]. It also appears that many parameters play a role in how the deactivation takes place. The presence of water during the sulfur exposure and the temperature at which the exposure to sulfur takes place seem to play a significant role in terms of catalyst deactivation [32,34]. Hammershøi et al. have shown that sulfur exposure of Cu-CHA SCR catalysts results in both reversible and irreversible catalyst deactivation. At temperatures around 400°C the deactivation is partly reversible and partly irreversible [33].

2.3 Biofuels

In order to reduce the impact the transport sector has on the environment and human health, a strive for more substantial use of biofuels is seen. Many biofuels can fully or partially substitute existing fossil fuels. Several liquid biofuels can substitute diesel, HVO and FAME are two examples of that type of biofuels. Both these fuels are based on vegetable oils or animal fats, however, the process used to up-grade the raw material to fuel differs for the two fuels. FAME is the one of the two fuels that is referred to as biodiesel. The process used to produce FAME is transesterification of the fat or oil with methanol (most commonly used) [35]. To produce HVO the oil or fat is hydrotreated, which gives a product referred to as renewable diesel fuel [36].
The standards that exist for biofuels are not as extensive as the standards for, e.g., diesel and petrol [35]. This causes irregular quality of the fuels depending on the raw material, which can vary substantially from country to country. This can also cause a more rapid deactivation of the catalysts due to higher content of various catalyst poisons in the fuel.

Chapter 3

Experimental methods

3.1 Catalyst samples

The results presented in this thesis are based on experiments performed on two different main types of catalysts, the copper exchanged zeolite and the vanadia-based catalyst. In paper I two slightly different Cu-SSZ-13 catalysts, denoted catalyst A and B, were used and in paper II one vanadia-based catalysts supported on TiO_2 and promoted by WO_3 was used. The catalysts were provided by external parties.

The difference between catalyst A and B in paper I is quite small, catalyst B has a slightly lower washcoat loading and a slightly higher copper content in the washcoat. Catalyst A was used for lab-aging while catalyst B was used for engine-aging.

In paper II where the vanadia-based catalyst was studied, one sample was taken from a heavy-duty vehicle that was fuelled by HVO, a second sample came from the same type of vehicle but the fuel used to power this vehicle was FAME. A fresh reference sample with the same composition as the field-aged samples was also included. The HVO and FAME samples experienced field-operation in EURO V systems without oxidation catalyst or particulate filter between the engine and the SCR catalyst. The reason to exclude the oxidation catalyst and filter is that the SCR catalysts are exposed to the engine out exhaust. This, however, most likely causes significant differences in catalytic performance between the inlet and the outlet of the SCR catalyst. Therefore, one sample core from the inlet section of the field-aged SCR catalysts and one sample core from the outlet section of theses catalysts were taken. The samples are denoted according to the fuel used and its original location in the SCR catalyst, e.g. FAMEin is a sample taken

from the inlet section of the SCR catalyst used in the FAME powered vehicle.

3.1.1 Sulfur deactivation

The fresh Cu-SSZ-13 catalyst samples of Catalyst A were subjected to sulfur in the form of SO_2. As mentioned previously this was performed in lab-scale. The aim was to investigate how the temperature during sulfur exposure impacts the degree of deactivation. Four different temperatures during sulfur exposure were investigated, 220, 280, 350 and 400°C, and the SCR activity of the catalysts was tested before and after sulfur exposure. The total amount of sulfur that passed the catalyst during lab-aging was 34 g/dm^3 Catalyst B was subjected to deactivation in a vehicle, which means that several assumptions must be made to calculate the amount of sulfur that passed the catalyst. The assumptions made in this study regarded fuel consumption, oil consumption and sulfur content in both fuel and oil. The calculated sulfur exposure (depending on catalyst volume and distance) was 8 mg/(dm^3 SCR catalyst and 100 km). To be able to compare Catalyst A and B, one lab-scale experiment at 280°C was performed for Catalyst B as well. It should also be pointed out that the conditions for vehicle and lab-scale aging differs since, for example, no NH_3 is present during aging in lab-scale whereas NH_3 is present during vehicle aging. The temperature is lower and constant during lab-aging, while the temperature constantly varies during vehicle aging. The concentration of sulfur is much higher in the lab-scale aging and the time that the sample is subjected to the poison is much shorter than for the vehicle aged sample.

3.2 *Ex situ* catalyst characterization

3.2.1 X-ray flourescence (XRF)

X-ray flourescence is used to determine the elemental composition of a sample. In paper I, XRF is used to determine and semi-quantitatively determine the elemental composition of the fresh and deactivated catalyst samples. The samples were cut into an inlet and an outlet part to detect differences between the two. The sample was mixed with a binder and ground into a fine powder that was dried and then pressed to a pellet.
The sample pellet was then subjected to X-rays that excite an electron from one of the inner orbitals of the atom, which in turn lead to that an electron in a higher orbital

moves to the lower orbital to fill the gap by emitting a photon of lower energy than the X-ray it was subjected to [37]. The intensity and energy of the emitted photons are measured which gives a quantitative measurements on the elements detected.
It should be pointed out that this method do not quantify the amount of sulfur in the sample exactly correct since no reference is taken, however it works well for comparisons between the different samples.

3.2.2 Nitrogen physisorption

To detect deactivation in the form of pore collapse and fouling the specific surface area could be determined. This is performed by nitrogen physisorption and this method is used in paper II. The measurement is performed by measuring the volume of nitrogen that is adsorbed/desorbed on the surface of the sample at 77 K at different pressures to form adsoption and desorption isotherms. To calculate the surface area from the physisorption measurements, a theoretical method is needed, the one used here is the BET method [38]. To use this method some assumptions are needed; (1) ideal behaviour of nitrogen gas molecules, (2) a monolayer of nitrogen is formed on the surface of the sample, (3) all sites on the sample surface are equal, (4) no interaction between adsorbed nitrogen molecules, and (5) the adsorbed nitrogen molecules do not move on the surface.

3.2.3 X-ray photoelectron spectroscopy (XPS)

X-ray photoelectron spectroscopy is an analysis method used to measure and quantify the elemental composition of the surface of a sample. In paper II the surface is defined as the top 4-5 nm of the sample. The method can also be used to identify the chemical and electronic states of the elements found on the surface. The spectra used to determine the above mentioned elemental properties are obtained by irradiating the sample with monochromatic X-rays while measuring the number of photoelectrons that escape from the surface of the sample and the kinetic energy of these electrons, see an example in Figure 4.2. Each element has core electrons with unique binding energies which makes it possible to identify almost all elements, hydrogen and helium are the two elements that are difficult to detect with this technique.

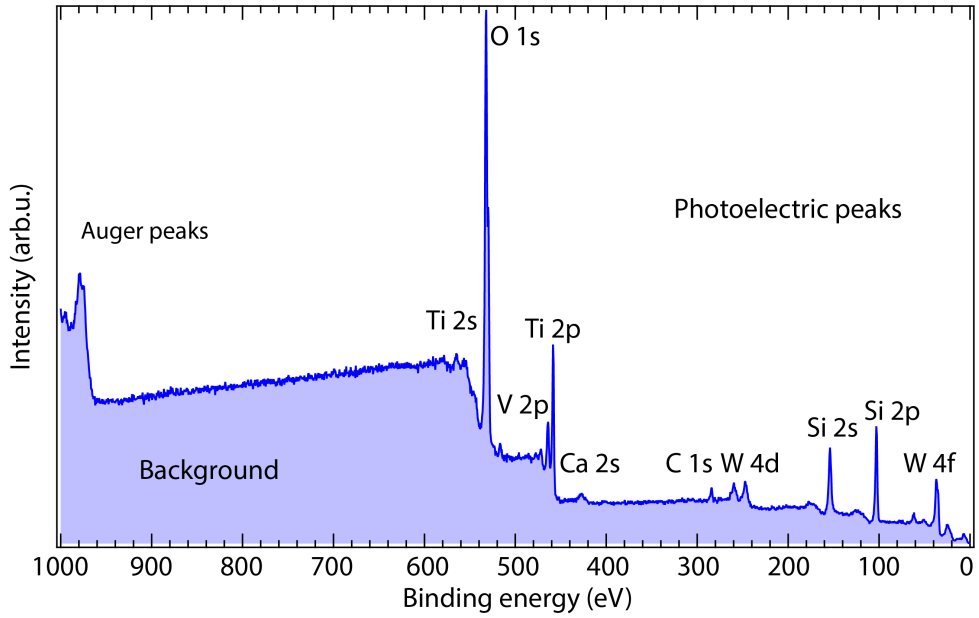

Figure 3.1: XPS spectrum of a V_2O_5-WO_3/TiO_2 SCR catalyst.

3.3 *In situ* catalyst characterization

3.3.1 Evaluation of the Cu-SSZ-13 catalyst in a gas flow reactor

The gas flow reactor used for the experiments described in this section (except for the SO_2 experiments that are performed in the system described in the next section) consists of a horizontal quartz tube heated by a furnace. Bronkhorst Hi-Tech gas flow controllers were used to control the gas flow and a CEM (controlled evaporator and mixer) system from the same manufacturer was used to provide the feed with water. The effluent gases were detected using an AVL Fourier transform infrared spectrometer (FTIR). The temperature was monitored with thermocouples positioned in the inlet and outlet of the catalyst sample.

Catalyst A was evaluated according to Figure 3.2.The samples were first exposed to a degreening procedure where the sample was subjected to 10 vol.-% O_2, 5 vol.-% H_2O and argon as balance (base feed) at 500°C for 1 h. Before the activity was evaluated, at both temperatures an ammonia saturation step was performed to be able to compare the total ammonia storage ability of the samples. The activity test protocol can be seen in Table 3.1. The activity of the fresh sample was measured by performing standard SCR, NO_2-rich SCR and fast SCR tests at two temperatures, 220 and 280°C.

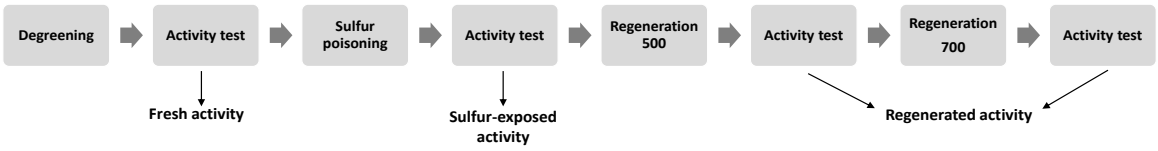

Figure 3.2: Experimental procedure for Catalyst A (Paper I).

The sulfur poisoning step in the experimental procedure, Figure 3.2, was performed by subjecting the sample to SO_2 for 8 hours at a constant temperature (220, 280, 350 or 400°C). The space velocity used for the sulfur poisoning step was 60,000 h^{-1} and the composition of the gas feed was the base feed plus 50 vol.-ppm SO_2.

Table 3.1: Activity test procedure. GHSV: 120,000 h^{-1} with base feed. The procedure was performed at both 220 and 280°C.

Step	NO (vol.-ppm)	NO_2 (vol.-ppm)	NH_3 (vol.-ppm)	Description
1	1000	0	0	Ref. NO_x concentration standard SCR
2	500	500	0	Ref. NO_x concentration fast SCR
3	250	750	0	Ref. NO_x concentration NO_2-rich SCR
4	0	0	0	N_2
5	0	0	1000	Saturation with NH_3 and ref. NH_3 conc.
6	1000	0	1000	Standard SCR activity
7	250	750	1000	NO_2-rich SCR activity
8	500	500	1000	Fast SCR activity
9	1000	0	0	Removal of NH_3 from the surface and ref. NO concentration

Two regeneration steps were performed, the first one at 500°C for 30 min and the second one at 700°C for 30 min. The samples were subjected to base feed at a space velocity of 120,000 h^{-1}. The two temperatures were chosen as a realistic deSO_x temperature that could be achieved in a heavy-duty vehicle without too high fuel penalty (500°C) and as a temperature where most or all sulfur would be desorbed and the

activity completely regained according to literature for similar catalysts [39, 40].

SCR reactions

The type of SCR reaction (standard, fast and NO_2-rich) which dominates in the SCR catalyst depends on the NO_2/NO_x ratio. For low NO_2/NO_x ratios or in absence of NO_2 in the feed, the dominating reaction that takes place over the catalyst is the standard SCR reaction described by equation 2.1, which is repeated below.

$$4NO + 4\mathrm{NH_3} + \mathrm{O_2} \rightarrow 4\mathrm{N_2} + 6\mathrm{H_2O}$$

In the new Euro VI systems, an oxidation catalyst is placed up-stream of the SCR catalyst which can lead to oxidation of NO to NO_2, which in turn results in a higher NO_2/NO_x ratio. The dominating SCR reaction that takes place over the SCR catalyst during these conditions is called the fast SCR reaction and is described by equation 2.2 and repeated below.

$$2NO + 4\mathrm{NH_3} + 2\mathrm{NO_2} \rightarrow 4\mathrm{N_2} + 6\mathrm{H_2O}$$

If the NO_2/NO_x ratio is higher than one, two reaction routes, described below in equation 3.1 and 3.2 [17], dominate.

$$8\mathrm{NO_2} + 6\mathrm{NH_3} \rightarrow 7\mathrm{N_2O} + 9\mathrm{H_2O} \tag{3.1}$$

$$4\mathrm{NO_2} + 4\mathrm{NH_3} + \mathrm{O_2} \rightarrow 4\mathrm{N_2O} + 6\mathrm{H_2O} \tag{3.2}$$

The gas feed composition during the tree types of SCR experiments are stated in Table 3.1.

SO_2 oxidation

The reactor system used for the SO_2 oxidation experiments is the same as used to evaluate the catalytic properties of the vanadia-based catalysts and it is described in the following section. Due to gas flow limitations, the GHSV used for the SO_2 oxidation experiments was 33,700 h^{-1}. The gas composition was 100 vol.-ppm SO_2, 8 vol.-% O_2 and argon as balance. The experiment was conducted in temperature steps of 50°C from

200 to 500°C and the effluent gases were detected by a gas-phase FTIR spectrometer (MKS 2030 HS). The remaining sulfur on the sample was measured by a sulfur analyzer (Leco CS230) after grinding and drying of the sample at 105°C.

3.3.2 Calculations

NH_3 storage

To calculate the total ammonia storage at respective test temperature, equation 3.3 was used

$$n_{NH_3} = (y_{NH_3,in} \cdot t - \int_0^t \mathrm{y}_{NH_3,out}\mathrm{d}t) \cdot \frac{v_{tot} \cdot P_{tot}}{R \cdot T} \tag{3.3}$$

where n_{NH_3} is the amount in mol of NH_3 stored on the catalyst, $y_{NH_3,in}$ is the volume fraction of NH_3, obtained by the FTIR, t is the time in seconds, T is the temperature in Kelvin, R is the gas constant 8.314 [Pa $m^3mol^{-1}K^{-1}$], v_{tot} is the total volumetric flow rate [m^3s^{-1}] and P_{tot} is the total pressure in pascal. The part of equation 3.3 within brackets comes from step 5 in Table 3.1 by plotting NH_3 concentration versus time and integrating between the inlet and outlet NH_3 concentration. The amount of desorbed/adsorbed SO_2 in the SO_2 oxidation experiment is quantified in a similar way.

Apparent rate constant

To be able to compare the activity of the differently treated catalysts A and B, the apparent rate constant was determined by equation 3.4 for the standard SCR reaction.

$$-k = \frac{F_{NO_x,in}}{c_{NO_x,in} \cdot v} ln(1 - \frac{X}{100}) \tag{3.4}$$

where k is the apparent rate constant in s^{-1}, X is the NO conversion in percent, $F_{NOx,in}$ is the molar flow rate of NO_x in the feed [mol s^{-1}], $c_{NOx,in}$ is the concentration of NO_x in the feed [mol dm^3] and V is the volume [dm^3]. The reaction order was assumed to be 1^{st} order with respect to NO_x and 0^{th} order with respect to NH_3. The dependence on the ammonia concentration is not actually zero but it is weaker than first order. The error is however the same for all samples since the experiments are performed at the same conditions. This means that the error cancels out when comparing the samples.

Overall sulfur capture

In paper I the overall sulfur capture (OASC) was defined according to equation 3.5

$$OASC = \frac{amount\ sulfur\ captured\ by\ the\ catalyst}{total\ sulfur\ throughput\ of\ catalyst} \cdot 100\ [\%] \tag{3.5}$$

How to calculate the sulfur throughput of the vehicle aged catalysts was described in section 3.1.1.

3.3.3 Evaluation of the vanadia-based catalyst in gas flow reactor

The gas flow reactor used for the experiments in this section, and the SO_2 experiments in the previous section, is slightly different to the one described and used for conduction the experiments on the Cu-SSZ-13 catalyst. The reactor consist of a quartz tube heated by a resistive heating coil. The gas flow is controlled by Bronkhorst Hi-Tech gas flow controllers and a CEM system from the same producer controls the water dosing. Thermocouples placed in the center and front of the catalyst are used to monitor any exotherms and controlling the heating system, respectively. The product gases are detected with an internally calibrated FTIR spectrometer, which means that a molecule without a net-change in dipole moment as it vibrates or rotates, can not be detected. One example of such a molecule is N_2.
The experiments conducted for the vanadium catalyst in this set up were NH_3-SCR, NH_3 oxidation and NH_3-TPD in that order. The space velocity was the same for all experiments, 40,000 h^{-1}.

NH_3-SCR

The type of SCR experiments conducted in this section was the standard SCR experiment. The dominating SCR reaction that takes place in these experiments is described in equation 3.3.1. No degreening of the vanadia-based catalyst samples were performed before NH_3-SCR experiments since such a procedure potentially could remove contaminants from the surface of the samples, which is not desired in this deactivation study. The gas composition used in these experiments were as follows, 400 vol.-ppm NH_3, 400 vol.-ppm NO, 8 vol.-% O_2, 5 vol.-% H_2O and argon balance. The experiments were performed in a temperature ramp from 500 to 100°C with a 5°C/min cooling.

NH_3 oxidation

To detect if the selectivity of NH_3 oxidation to the preferred NH_3 SCR reaction over the field-aged catalysts has changed, an ammonia oxidation experiment was performed. The NH_3 oxidation experiment was conducted after the SCR experiment by subjecting the sample to 400 vol.-ppm NH_3, 8 vol.-% O_2, 5 vol.-% H_2O and argon as balance while performing the same temperature ramp as for the SCR experiments.

NH_3-TPD

By performing temperature programmed desorption (TPD) experiments it is possible to detect changes in number and type of active sites. In the NH_3-TPD experiment, the sample is first saturated with NH_3 at 150°C by flowing 400 vol.-ppm NH_3 in argon over the sample for 45 minutes. When the sample was saturated with NH_3, the sample was exposed to argon to remove loosely bound NH_3 from the surface of the catalyst sample. The temperature was then linearly increased to 500°C at a rate of 20°C/min while the desorbed amount of NH_3 continuously was measured.

Chapter 4

Results and Discussion

This thesis is based on two independent studies presented in paper I and II, respectively. In the study presented in paper I, the effect of SO_2 on the low-temperature activity of a Cu-SSZ-13 SCR catalyst was studied. Specifically the effect of the SO_2 exposure temperature and the influence of the NO_2/NO_x ratio on the activity of the catalyst was investigated. In addition, two different regeneration temperatures were compared and engine-aged samples were tested and compared with lab-aged samples. In paper II, the impact of powering the vehicle with two different biofuels, FAME and HVO, on the catalytic performance of a commercially available vanadia-based SCR catalyst used in Euro V heavy-duty vehicles before and after field-operation, was investigated.

4.1 Sulfur exposure of the Cu-SSZ-13 SCR catalyst

To compare the activity of a fresh sample with the samples exposed to sulfur, standard, fast and NO_2-rich SCR experiments were performed. In Figure 4.1 the activity results at 280°C for the fresh sample (left) and the sample exposed to SO_2 (right) at 280°C are shown. The graphs show the outlet concentrations of NO, NO_2, N_2O and NH_3 in vol.-ppm. The inlet gas composition was 1000 vol.-ppm NO_x, 1000 vol.-ppm NH_3, 10 vol.-% O_2, 5 vol.-% H_2O with a space velocity of 120,000 h^1.

It can clearly be seen in Figure 4.1 that subjecting the catalyst to SO_2 is detrimental in terms of activity for NO_x reduction. The figure also shows that the impact of SO_2 exposure differs for the three different types of SCR reactions tested. The standard SCR reaction is most severely affected by the SO_2 exposure while the impact on the fast SCR reaction is minor. The impact of SO_2 is also dependent on the SO_2 exposure

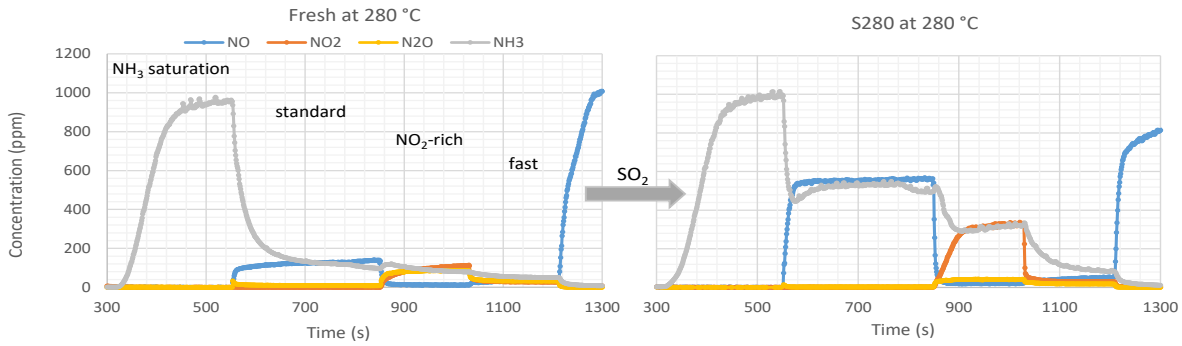

Figure 4.1: Outlet concentrations of NO, NO_2, N_2O and NH_3 during NH_3 exposure and standard SCR, NO_2-rich SCR and fast SCR activity tests of a fresh Cu-SSZ-13 SCR catalyst sample (left) and a sample exposed to SO_2 at 280°C (right) (Paper I).

temperature, which is evident from Figure 4.2 where the relative rate constant for the standard SCR reaction for each sample at two different temperatures is presented. The relative rate constant is a comparison between the rate constant of the samples exposed to SO_2 and the fresh sample, expressed in percent.

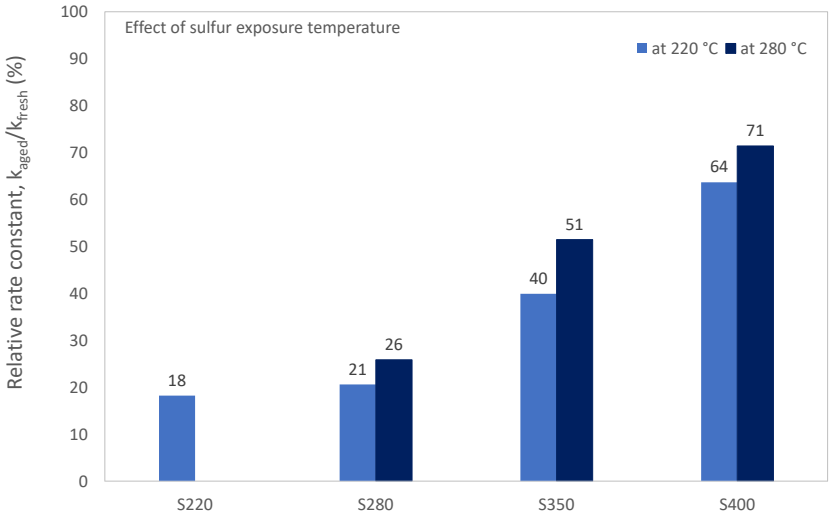

Figure 4.2: Relative rate constant at 220 and 280°C for Cu-SSZ-13 SCR catalyst samples exposed to SO_2 at 220, 280, 350 and 400°C (Paper I) .

The results in Figure 4.2 show that increasing the SO_2 exposure temperature results in an increased relative rate constant, which is in line with the results for for Cu-SSZ-

13 by Wijayanti et al. [34]. Not only the activity for NO_x reduction is impacted by SO_2 exposure, the N_2O selectivity is also affected. The results presented in Figure 4.3 show how the N_2O selectivity changes with type of SCR reaction and SO_2 exposure temperature. It can be seen that a higher NO_2/NO_x ratio results in increased N_2O selectivity, which is in agreement with what Toops et al. have found [41].

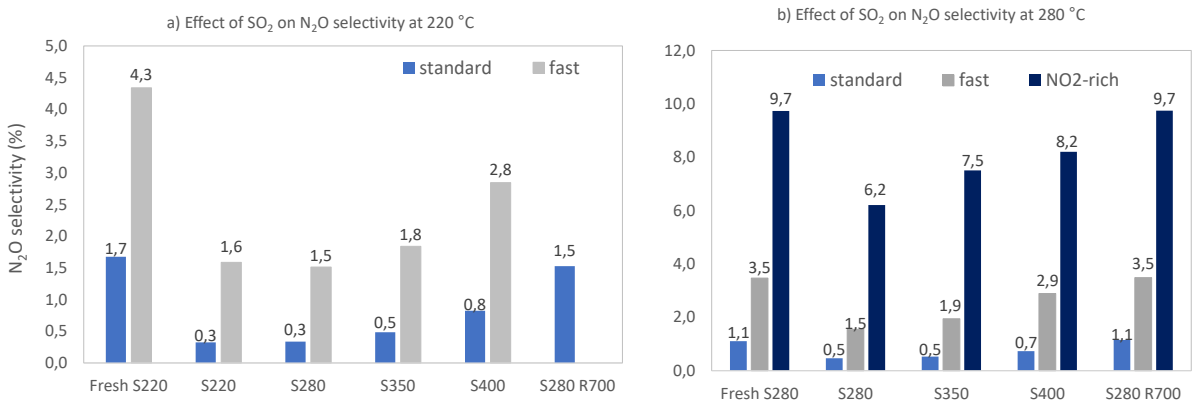

Figure 4.3: N_2O selectivity of fresh, SO_2-exposed and regenerated Cu-SSZ-13 SCR catalyst samples during a) standard and fast SCR reaction conditions at 220°C, and b) standard, fast and NO_2-rich SCR reaction conditions at 280°C (Paper I).

When the decrease in N_2O selectivity is compared to the decrease in NO_x reduction it can be seen that the low-temperature SO_2 exposure results in a decrease of similar magnitude for both parameters. However, at the higher SO_2 exposure temperatures the decrease in N_2O selectivity is proportionally higher then the decrease in NO_x reduction. This could be explained by the presence of two different types of Cu^{2+} sites in the zeolite, one type of sites in the 8-membered ring (8MR) and one type in the 6-membered ring (6MR) [42–44]. The Cu^{2+} sites in the 6MR have been proposed to be responsible for the SCR reaction while the site in the 8MR have been proposed to be responsible for oxidation as well as SCR reactions. The two types of sites respond to SO_2 exposure differently where the sites in the 8MR are more severely impacted which is caused by the weaker interaction between copper and the zeolite. At the higher exposure temperatures, less sulfur adsorbs on the catalyst surface during the SO_2 exposure (see table 4.1) resulting in less deactivation of the sites in the 6MR and a relatively higher decrease in N_2O selectivity in comparison to the decrease in NO_x reduction.

For the samples exposed to SO_2 at lower temperatures, the ammonia storage capacity seems to be unaffected even though the SCR activity is severely affected 4.4. This could be caused by storage of ammonia as ammonium sulfate-like species by the sulfur blocking the active copper sites. However, at higher exposure temperatures, the storage capacity increases after sulfur exposure with the most substantial increase at the highest exposure temperature. This is likely caused by the fact that at higher temperatures more of the adsorbed SO_2 is oxidized to SO_3 which in turn more readily reacts with the copper sites to form acidic sulfate sites where additional NH_3 can be stored. At the regeneration temperature of 700°C, the acidic sulfate species decompose which results in a similar NH_3 adsorption capacity as for the fresh sample.

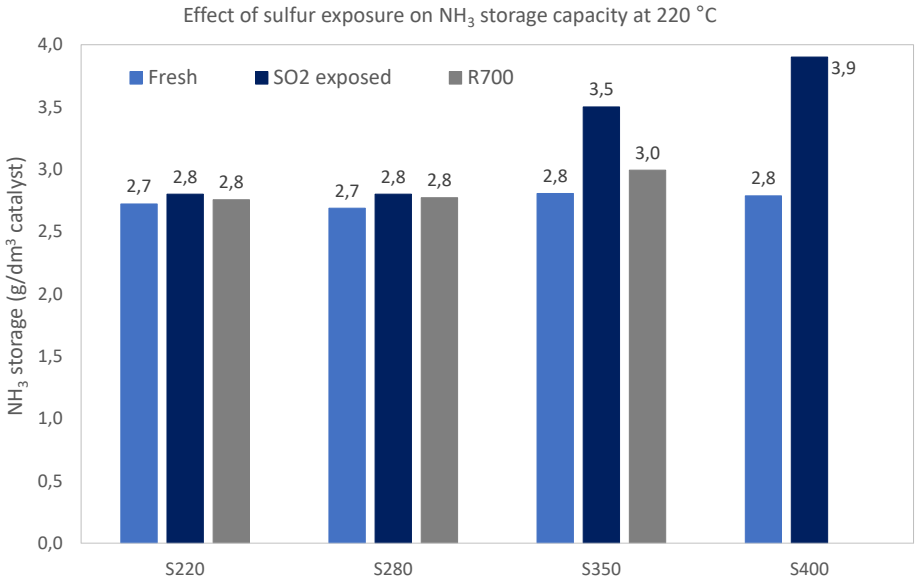

Figure 4.4: Total NH_3 storage at 220°C for fresh, SO_2 exposed and regenerated Cu-SSZ-13 SCR catalyst samples (Paper I).

The sulfate species that can store additional NH_3 were found to be formed above 300°C [45]. The trend with increased NH_3 storage for samples exposed to SO_2 at higher temperatures was not seen when the experiments were performed at 280°C.
To investigate whether or not SO_2 can form SO_3 over the Cu-SSZ-13 catalyst, SO_2 oxidation experiments were performed. The results of these experiments are shown in Figure 4.5. The sulfur balance is defined as the amount of sulfur at the outlet of the reactor system, in the form of SO_2 and SO_3 combined, subtracted from the inlet amount

of sulfur, in the form of SO_2.

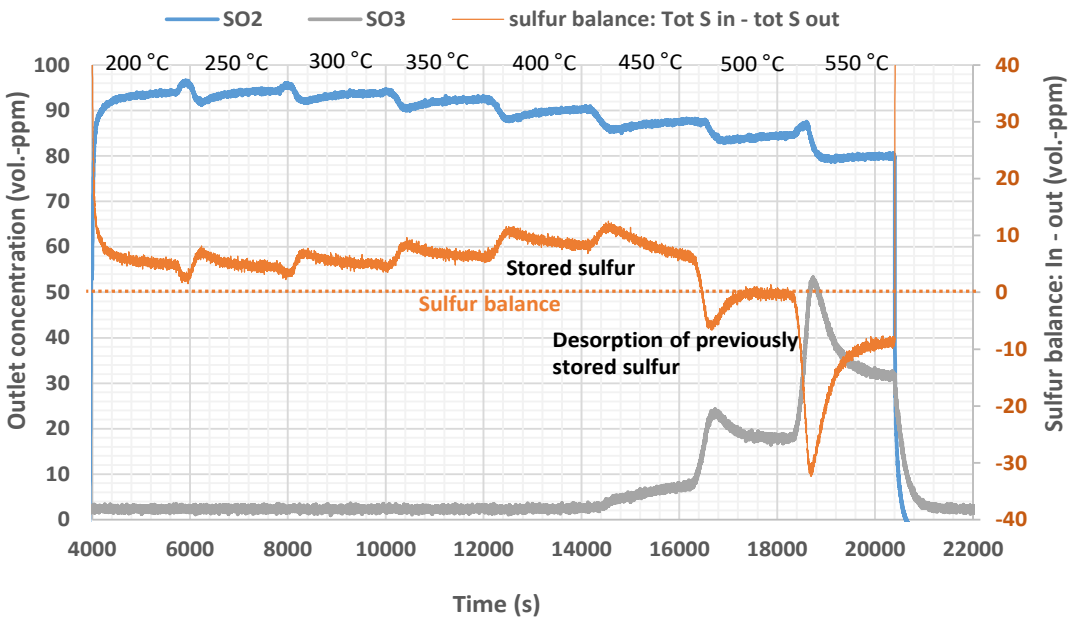

Figure 4.5: Outlet concentrations of SO_2 and SO_3, and temperature during an SO_2 oxidation experiment over the Cu-SSZ-13 SCR catalyst. Inlet concentrations: 100 vol.-ppm SO_2, 8 vol.-% O2, space velocity of 33,700 h^{-1} (Paper I).

The figure shows that below 500°C, the sulfur balance is positive which means that some sulfur is stored on the catalyst or on the walls of the quartz reactor tube. How this sulfur is stored is not revealed by this experiment. However, when the temperature reaches 450°C, SO_3 is detected by the gas phase FTIR analyzer. The SO_3 concentration never reaches stable levels and this is likely due to that SO_3 adsorbs on surfaces more strongly than SO_2. At temperatures above 500°C, the sulfur balance is negative, which indicates that some of the sulfur adsorbed at lower temperatures desorbs above 500°C. After exposing the Cu-SSZ-13 SCR catalyst for SO_2 and O_2 at the highest temperature, the remaining amount of sulfur on the catalyst sample was determined in two different ways. To calculate the remaining amount of sulfur from the data collected by the FTIR analyzer, the SO_2 and SO_3 concentrations versus time were integrated. The second way to retrieve the concentration of sulfur on the sample after the experiment was to perform a sulfur analysis, both methods showed that the concentration of sulfur on the sample after the experiment was 0.14 wt.-%.

The sulfur content of some of the SO_2 exposed samples, regenerated samples and fresh samples are presented in Table 4.1. From the table, it can be seen that the sample exposed to SO_2 at 350°C (S350) contains much less sulfur than the sample exposed to SO_2 at 280°C (B-S280), although the catalyst formulations differ slightly (S350 is catalyst A and B-S280 catalyst B). It can also be seen that regeneration at 700°C results in almost complete removal of sulfur which was the aim when choosing that high regeneration temperature. In addition to sulfur, also increased levels of P, Zn and Ca were found in the engine-aged (E-A) samples, which most likely have an impact on the catalytic properties of these samples. It can also be seen that the sulfur levels are much lower for the engine-aged samples. This is due to that the engine-aged and lab-aged samples have been treated rather differently where the engine-aged samples have been subjected to lower sulfur levels and exposed to SCR conditions and high temperatures.

4.1.1 Engine aged Cu-SSZ-13 SCR catalyst

As mentioned in the previous section, the engine-aged Cu-SSZ-13 catalyst samples contain phosphorous, zinc and calcium in addition to the investigated catalyst poison sulfur. These additional catalyst poisons have an impact on the SCR activity of the catalyst, which can be seen in Figure 4.6. The rate constant for the standard SCR reaction at

Table 4.1: Sulfur content in samples analyzed by XRF. I=inlet of the catalyst, O=outlet of the catalyst

Sample	Sulfur content [wt-%]
Fresh	<0.005
S220, R700	0.03
S280, R700	0.03
S350	0.27 (I), 0.3 (O)
B-Fresh	<0.005
B-S280	0.43
B-S280, R700	0.06 (I), 0.09 (O)
E-A in	0.11
E-A in, R700	0.08
E-A out	0.07

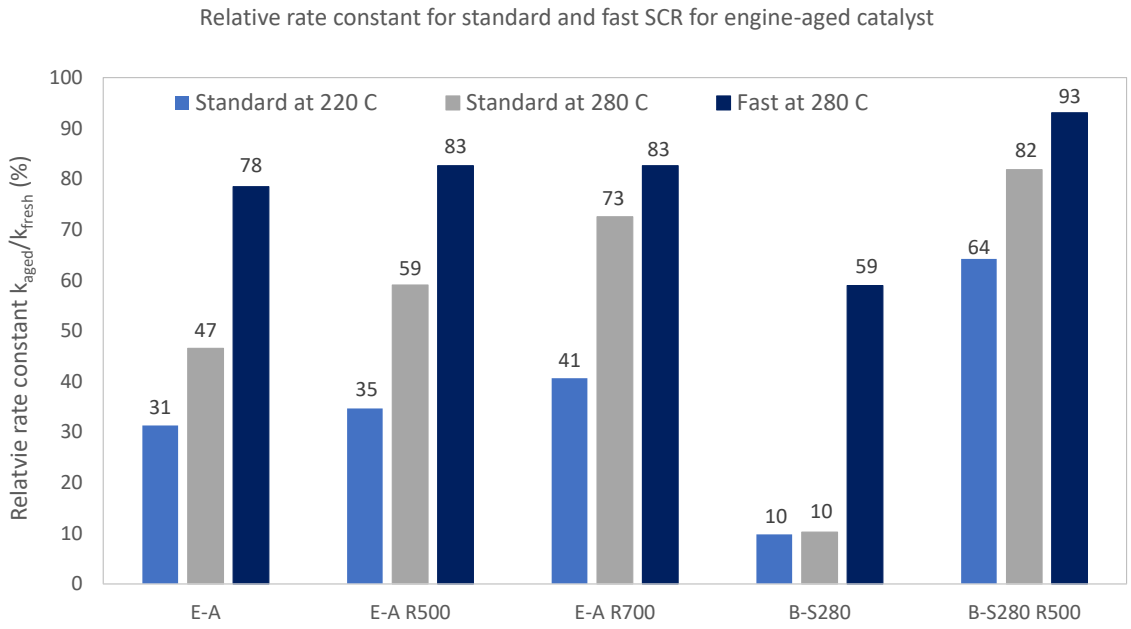

Figure 4.6: Relative rate constants for engine-aged and lab aged Cu-SSZ-13 SCR catalyst samples during the at 220 and 280°C. Inlet concentrations during the test: 1000 vol.-ppm NO_x and NH_3, 10 vol.-% O_2, 5 vol.-% H_2O and a space velocity of 120,000 h^{-1} (Paper I).

220°C has decreased significantly for the engine-aged catalyst compared to the fresh catalyst. The rate constant at 280°C is also lower compared to the fresh catalyst, however not to the same extent as at the lower temperature. It can also be seen in the figure that the fast SCR reaction is considerably less affected than the standard SCR reaction. Moreover, the catalyst exposed to SO_2 at 280°C in the flow reactor is more severely deactivated than the engine-aged catalyst. However, after regeneration at 700°C the activity of the lab aged catalyst is restored whereas the engine-aged catalyst only slightly regains activity.

When it comes to N_2O selectivity, shown in Figure 4.7, the engine-aged Cu-SSZ-13 SCR catalyst shows a small decrease and the lab-aged catalyst shows a considerable decrease in N_2O selectivity for the standard SCR reaction conditions at 220°C. For the fast SCR conditions at the same temperature, the difference in N_2O selectivity between the lab-aged and engine-aged samples is more substantial. At 280°C, the N_2O selectivity of the engine-aged catalyst is higher compared to the fresh catalyst for all SCR reaction conditions, while the N_2O selectivity for the lab-aged catalyst is is similar or lower

compared to the fresh catalyst.

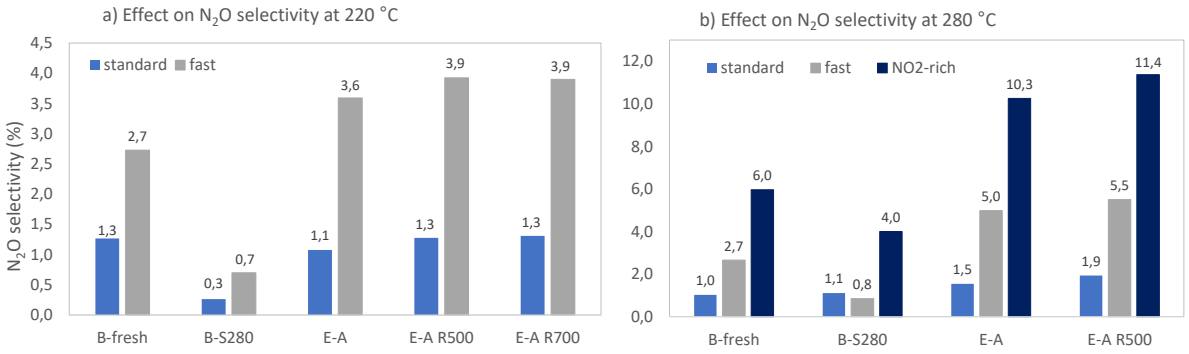

Figure 4.7: N_2O selectivity of the inlet part of the engine-, lab-aged and regenerated Cu-SSZ-13 SCR catalysts during a) the standard and fast SCR reactions at 220°C, and b) the standard, fast and NO_2-rich SCR reactions at 280°C. Inlet concentrations during the test: 1000 vol.-ppm NO_x and NH_3, 10 vol.-% O_2, 5 vol.-% H_2O and a space velocity of 120,000 h^{-1} (Paper I).

As was seen in Figure 4.4 all samples had similar or an increased NH_3 storage capacity after SO_2 exposure as compared to the fresh sample. The engine-aged sample, however, showed the opposite result where the NH_3 storage capacity was slightly decreased after SO_2 exposure. After regeneration a slight increase in NH_3 storage capacity was observed.

4.2 Deactivation of the vanadia-based catalyst from the use of biofuels

The vanadia-based SCR catalyst samples were tested before and after field-aging in two heavy-duty vehicles fuelled with HVO and FAME, respectively. The catalytic activity was tested in standard SCR experiments with an inlet gas composition consisting of 400 vol.-ppm NO, 400 vol.-ppm NH_3, 8 vol.-% O_2 and 5 vol.-% H_2O with argon as balance. The experiments were performed in a temperature ramp of 5°C/min from 500 to 100°C with a space velocity of 40,000 h^{-1}. The results show that the NO_x conversion over the catalyst samples taken from the vehicle powered by FAME is severely affected, see Figure 4.8.

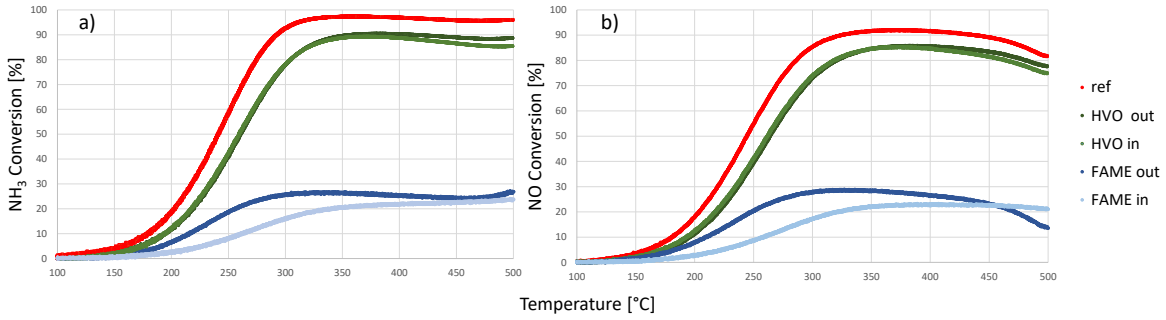

Figure 4.8: NH_3 (a) NO (b) conversion during standard-SCR experiments over the fresh and field-aged vanadia-based SCR catalysts. Fresh (red), HVOin (light green), HVOout (dark green), FAMEin (light blue) and FAMEout (dark blue). The samples were exposed to 400 vol.-ppm NO, 400 vol.-ppm NH_3, 8 vol.-% O_2 and 5 vol.-% H_2O with Ar as balance (Paper II).

The inlet and outlet samples of the catalyst field-aged with FAME as fuel show similar SCR activity at the higher temperatures, however at the lower temperatures the activity of the FAMEin sample is lower. This could be due to a high coverage of soot on the inlet of the sample. It could also be due to a high concentration of alkali metals on the FAMEin sample that was seen from the XPS analysis, see Table 4.2. The XPS analysis also reveal that the catalyst samples taken from the vehicle fuelled with HVO have the same amount of carbon (or higher) on the inlet and outlet samples as the catalyst samples taken from the vehicle fuelled with FAME. However, the HVO samples show almost as high SCR activity as the fresh catalyst. This indicates that soot is not the cause of the decrease in SCR activity for the FAME samples.

Table 4.2: The surface atomic concentrations of the fresh and field-aged vanadia-based catalysts as obtained by XPS analysis.

Sample	Ti	V	W	Si	O	C	Ca	Mg	Zn	P	K	Na
Fresh	6.8	0.6	1.5	20	65	6.2	-	-	-	-	-	-
HVO in	4.9	0.4	0.9	11	52	26	0.8	1.2	0.1	0.9	-	-
HVO out	7.0	0.5	1.4	15	61	13	0.9	-	-	0.1	-	-
FAME in	3.5	0.4	0.6	11	53	21	0.7	3.4	0.8	2.5	Yes	Yes
FAME out	6.3	0.5	1.0	17	65	7.8	1.0	-	0.2	0.8	Yes	-

From the XPS results it can be seen that the FAME inlet and outlet sample contains 0.8 and 0.2 at.% Zn, respectively. For the samples from the catalyst field-aged with HVO, only the inlet sample shows traces of Zn (0.1 at.%). Both the HVO and FAME samples contain Ca, the outlet section of both catalysts shows higher calcium concentrations than the inlet section (FAMEout 1.0 at.%, HVOout 0.9 at.%, FAMEin 0.7 at.%, HVOin 0.8 at.%). The FAME samples show traces of K while traces of sodium are found on the inlet section of the catalyst field-aged with FAME. The phosphorous content is higher for the FAME samples as well with a significant amount of 2.5 at.% of P on the FAME inlet sample. The corresponding concentration for the HVO inlet is 0.8 at.%. The differences in concentrations between the FAME and HVO could partly be explained by the difference in driving time for the two vehicles. The results from the NH_3 oxidation experiments show similar trends as the results from the standard SCR experiments. The activity for NH_3 oxidation decreases for both the HVO and FAME samples but considerably more for the FAME samples which is shown in Figure 4.9. A slightly larger difference between inlet and outlet for the FAME samples, when compared with the HVO samples, is also seen and this could be due to the presence of sodium on the inlet sample or the high concentration of phosphorous on the same sample. From the TPD results in Figure 4.10 it can bee seen that the amount of NH_3 stored on the samples from the catalyst field-aged with HVO as fuel is marginally lower compared to the fresh catalyst. However, the catalyst amount of stored NH_3 is considerably lower for the catalyst field-aged with FAME as fuel. Furthermore, the amount of stored NH_3 is higher for the inlet than for the outlet section of catalyst field-aged with FAME. The higher amount of stored NH_3 on the FAME inlet sample can be due to storage on acidic species, e.g. phosphate or sulfate.

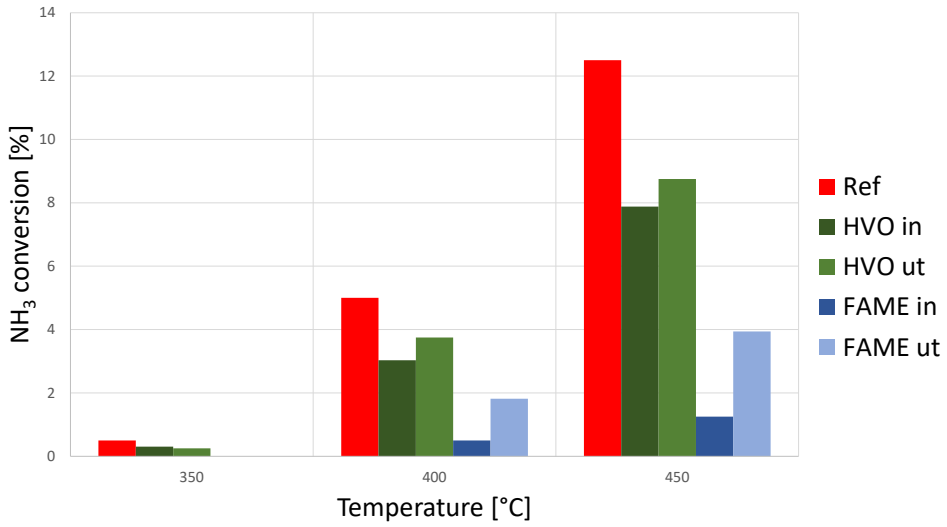

Figure 4.9: NH_3 conversion at 350, 400 and 450°C during NH_3-oxidation experiments over the inlet section of the fresh, and inlet and outlet sections of the field-aged vanadia-based catalysts. The samples were exposed to 400 vol.-ppm NH_3, 8 vol.-% O_2 and 5 vol.-% H_2O with Ar as balance (Paper II).

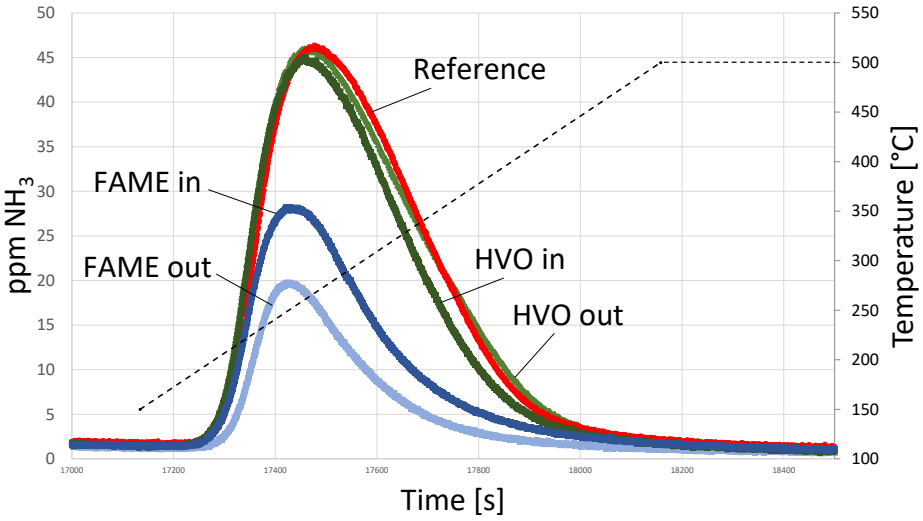

Figure 4.10: Outlet concentration of NH_3 during NH_3-TPD experiments for the fresh and field-aged vanadia-based catalysts. Fresh (red), HVOin (dark green), HVOout (light green), FAMEin (dark blue), FAMEout (light blue) and temperature (dotted black) (Paper II).

Chapter 5

Concluding remarks and Outlook

Deactivation of automotive catalysts is an important topic since long-term deactivation of these catalysts will lead to increased emissions of compounds that are detrimental to environment and human health. One example of such a compound is NO_x that is normally efficiently reduced by the SCR catalyst. In this thesis the deactivation of two different types of SCR catalysts has been studied.

The Cu-SSZ-13 SCR catalysts studied in paper I have high hydrothermal stablity, however this type of catalyst is sensitive to sulfur poisoning and consequently, the influence of sulfur exposure has been studied. More specifically the influence of temperature during SO_2 exposure on the low-temperature SCR activity was studied. It was shown that the lowest investigated exposure temperature led to the highest uptake of sulfur causing most severe deactivation. It has previously been seen by Wijayanti et al. that the deactivation after SO_2 exposure is most severe for standard SCR in comparison with fast and NO_2 rich SCR, and that is also seen in this study [34]. It was also shown, in paper I, that the selectivity for N_2O formation decreased after SO_2 exposure. However, the formation of N_2O increases with the NO_2/NO_x ratio which is in line with results reported by Toops et al., i.e. when the concentration of NO_2 in the feed is increased the selectivity towards N_2O also increases [41]. The engine-aged sample showed a decreased NO_x reduction ability and an increased selectivity towards N_2O formation which most likely is caused by poisons present in the fuel and engine-oil used in the vehicle.

Deactivation due to SO_2 exposure is a minor issue for the vanadia-based SCR catalyst studied in paper II since this type of catalyst does not take up sulfur to the same extent as the Cu-SSZ-13 catalyst. The amount and type of catalyst poisons that the catalyst is subjected to depend on the type of fuel and also the origin of the fuel. The in-

troduction of more biofuels into the vehicle fuel market could cause some problems due to non strict standards for these fuels leading to higher contents of catalyst poisons that could decrease the activity of the catalytic converters in the exhaust emission systems. In paper II the impact on a vanadia-based SCR catalyst from the use of two different biofuels has been investigated. The two fuels used were HVO and FAME and from paper II it can be seen that the use of FAME is much more detrimental to the SCR catalyst than the use of HVO. Both the activity for NO_x reduction and NH_3 oxidation decrease substantially after field-aging with FAME as fuel. Also the NH_3 storage capacity decreased considerably after field-aging in the vehicle fuelled by FAME. The deactivation of the samples taken from the FAME fuelled vehicle is likely caused by the accumulation of P, Ca, Zn and Mg that were detected on the surface of those samples. These catalyst poisons most likely originates from the FAME fuel.

In this thesis the deactivation effect from sulfur and biofuels has been investigated but not only the catalyst poison itself is of interest when it comes to catalyst deactivation. The scale of the experiments does also impact the results. In paper I, lab scale experiments were performed with engine-aged samples, and it was shown that many more parameters are significant when studying an engine-aged sample in comparison to a lab-aged sample. It was also shown that many more catalyst poisons than sulfur are present. With that said it is important to conduct deactivation studies in accelerated experiments in-lab scale. However, it is also important to see the full picture by performing engine experiments as well and that is part of the future goals for this project, to perform experiments where all parts of the emission control system are present.

Acknowledgements

The research presented in this thesis was carried out at the Division of Applied Chemistry and the Competence Centre for Catalysis (KCK), Chalmers University of Technology, Göteborg, Sweden, during the period of July 2014 to March 2018. This work has been performed within the FFI program (38364-1), which is financially supported by the Swedish Energy Agency, Scania CV AB, AB Volvo and Haldor Topsøe A/S, and partly within the Competence Centre for Catalysis, which is hosted by Chalmers University of Technology and financially supported by the Swedish Energy Agency (22490-3), Chalmers and the member companies AB Volvo, ECAPS AB, Haldor Topsøe A/S, Scania CV AB, Volvo Car Corporation AB and Wärtsilä Finland Oy.

I would also like to thank:

My supervisor Magnus Skoglundh and co-supervisor Per-Anders Carlsson for your support and encouragement. I really do appreciate that you always take the time to discuss results or problems and that your doors are always open when guidance and feedback is needed.

Sandra Dahlin for being my partner in this project and for all the nice discussions and ideas we shared. And also for the time we spent together on trips and in the lab, I always enjoy working with you.

Lasse Urholm and Lennart Norberg for all your help in the reactor lab and all the fun times and laughs we shared so far.

Hanna Härelind for being a very supportive examiner and guide through my time in academia, your sharing of knowledge and experience is very much appreciated.

Frida Andersson, Ann Jacobsson and Lotta Petterson for administrative help and for all the great social events you have organized.

Anne Wendel for all the help with our common mischief, the ASAP 2020, and for always spreading joy.

My roomie, Carl-Robert, for beeing a great friend and colleague. Without you it would not be as much fun going to work.

Peter who contributed with Figure 2.2 in this thesis and who brightens my workdays, you are a great friend and colleague.

Present and previous colleagues at KCK and TYK for all the fun times on and off campus. A special thanks to: Andreas, Anna, Colin, David, Emma, Felix, Freddy, Giulio, Jacob, Johan, Leo, Linda, Maria, Milene, Natalia, Sam, Simone, Simone, Soran, Ting.

My girls that have been with me for a long time, I love you Maya, Maddie and Saba.

My Mom and Dad who has always supported me and helped me be the best I can, my brother and sister who I can always depend on, you mean the world to me. Also my second family, Susanne, Stefan, Aleksandra and Lydia, I'm so happy to have you in my life.

The person that told be to go for it when this position came up. The one who loves me and who I love limitless, the one person who have given me my two most precious treasures Sigrid and Rut, thank you for everything Simon (The pictures you send me everyday featuring our girls light up my day).

Johanna Englund, Göteborg, March 2018

Bibliography

[1] Regualtion No 595/2009, Official journal of the european union, 2009.

[2] European Commission, Reducing co2 emissions from passenger cars, 2018.

[3] C. Ding, L. Roberts, D. J. Fain, A. K. Ramesh, G. M. Shaver, J. James McCarthy, M. Ruth, E. Koeberlein, E. A. Holloway, and D. Nielsen, *International Journal of Engine Research*, 2016, **17**(6), 619–630.

[4] P. Mendoza-Villafuerte, R. Suarez-Bertoa, B. Giechaskiel, F. Riccobono, C. Bulgheroni, C. Astorga, and A. Perujo, *Science of The Total Environment*, 2017, **609**, 546 – 555.

[5] C. Bartholomew, *Applied Catalysis A: General*, 2001, **212**(1), 17–60.

[6] J. Moulijn, A. Van Diepen, and F. Kapteijn, *Applied Catalysis A: General*, 2001, **212**(1-2), 3–16.

[7] Y. Liu, Z. Liu, B. Mnichowicz, A. Harinath, H. Li, and B. Bahrami, *Chemical Engineering Journal*, 2016, **77**(3-4), 215–227.

[8] J. Ross, *Heterogeneous catalysis: fundamentals and applications*, 2012, p. 1.

[9] O. Kröcher and M. Elsener, *Applied Catalysis B: Environmental*, 2008, **77**(3), 215–227.

[10] S. Dahlin, M. Nilsson, D. Bäckström, S. L. Bergman, E. Bengtsson, S. L. Bernasek, and L. J. Pettersson, *Applied Catalysis B: Environmental*, 2016, **183**, 377–385.

[11] M. Klimczak, P. Kern, T. Heinzelmann, M. Lucas, and P. Claus, *Applied Catalysis B: Environmental*, 2010, **95**(1), 39–47.

[12] D. Nicosia, I. Czekaj, and O. Kröcher, *Applied Catalysis B: Environmental*, 2008, **77**(3), 228–236.

[13] H. Kamata, K. Takahashi, and C. Odenbrand, *Journal of Molecular Catalysis A: Chemical*, 1999, **139**(2-3), 189–198.

[14] L. Chen, J. Li, and M. Ge, *Chemical Engineering Journal*, 2011, **170**(2), 531–537.

[15] F. Castellino, S. Rasmussen, A. Jensen, J. Johnsson, and R. Fehrmann, *Applied Catalysis B: Environmental*, 2008, **83**(1-2), 110–122.

[16] P. L. Gabrielsson, Apr , 2004, **28**(1), 177–184.

[17] M. Devadas, O. Kröcher, M. Elsener, A. Wokaun, N. Söger, M. Pfeifer, Y. Demel, and L. Mussmann, *Applied Catalysis B: Environmental*, 2006, **67**(3), 187 – 196.

[18] A. Grossale, I. Nova, E. Tronconi, D. Chatterjee, and M. Weibel, *Journal of Catalysis*, 2008, **256**(2), 312 – 322.

[19] M. Iwasaki and H. Shinjoh, *Applied Catalysis A: General*, 2010, **390**(1), 71 – 77.

[20] N. Martin, M. Moliner, and A. Corma, *Chem. Commun.*, 2015, **51**, 9965–9968.

[21] R. Long and R. Yang, *Journal of the American Chemical Society*, 1999, **121**(23), 5595–5596.

[22] T. Komatsu, M. Nunokawa, I. Moon, T. Takahara, S. Namba, and T. Yashima, *Journal of Catalysis*, 1994, **148**(2), 427–437.

[23] S. Brandenberger, O. Kröcher, A. Tissler, and R. Althoff, *Catalysis Reviews - Science and Engineering*, 2008, **50**(4), 492–531.

[24] I. Bull, W.-M. Xue, P. Burk, R.S. Boorse, W.M. Jaglowski, G.S. Koermer, A. Moini, J.A. Patchett, J.C. Dettling, M.T. Caudle, US patent 7,610,662, 2009.

[25] J. H. Kwak, R. G. Tonkyn, D. H. Kim, J. Szanyi, and C. H. Peden, *Journal of Catalysis*, 2010, **275**(2), 187 – 190.

[26] S.I. Zones, US patent 4,544,538, 1985.

[27] D. Fickel and R. Lobo, *Journal of Physical Chemistry C*, 2010, **114**(3), 1633–1640.

[28] D. Nicosia, I. Czekaj, and O. Kröcher, *Applied Catalysis B: Environmental*, 2008, **77**(3), 228 – 236.

[29] J. Chen and R. Yang, *Applied Catalysis A: General*, 1992, **80**(1), 135 – 148.

[30] C. H. Bartholomew, *Applied Catalysis A: General*, 2001, **212**(1), 17 – 60.

[31] P. Velin, Spectroscopic characterisation of surface hydroxyls during methane oxidation, 2018.

[32] S. Dahlin, C. Lantto, J. Englund, B. Westerberg, F. Regali, M. Skoglundh, and L. J. Pettersson, *Catalysis Today*, 2018.

[33] P. S. Hammershøi, Y. Jangjou, W. S. Epling, A. D. Jensen, and T. V. Janssens, *Applied Catalysis B: Environmental*, 2018, **226**, 38 – 45.

[34] K. Wijayanti, K. Leistner, S. Chand, A. Kumar, K. Kamasamudram, N. W. Currier, A. Yezerets, and L. Olsson, *Catal. Sci. Technol.*, 2016, **6**, 2565–2579.

[35] G. Knothe, *Fuel Processing Technology*, 2005, **86**(10), 1059 – 1070.

[36] H. Aatola, M. Larmi, T. Sarjovaara, and S. Mikkonen, oct , 2008, **1**(1), 1251–1262.

[37] B. Beckhoff, B. Kanngiesser, N. Langhoff, R. Wedell and H.Wolff, *Handbook of Practical X-Ray Fluorescence Analysis*, 2006.

[38] S. Brunauer, P. H. Emmett, and E. Teller, *Journal of the American Chemical Society*, 1938, **60**(2), 309–319.

[39] D. Brookshear, J.-G. Nam, K. Nguyen, T. Toops, and A. Binder, *Catalysis Today*, 2015, **258**, 359–366.

[40] L. Zhang, D. Wang, Y. Liu, K. Kamasamudram, J. Li, and W. Epling, *Applied Catalysis B: Environmental*, 2014, **156-157**, 371 – 377.

[41] T. Toops, J. Pihl, and W. Partridge, *Funda-Mental and Applied Catalysis*, 2014, **15**(3), 97–121.

[42] L. Olsson, K. Wijayanti, K. Leistner, A. Kumar, S. Joshi, K. Kamasamudram, N. Currier, and A. Yezerets, *Applied Catalysis B: Environmental*, 2015, **174-175**, 212–224.

[43] L. Olsson, K. Wijayanti, K. Leistner, A. Kumar, S. Joshi, K. Kamasamudram, N. Currier, and A. Yezerets, *Applied Catalysis B: Environmental*, 2016, **183**, 394–406.

[44] J. Luo, D. Wang, A. Kumar, J. Li, K. Kamasamudram, N. Currier, and A. Yezerets, *Catalysis Today*, 2016, **267**, 3–9.

[45] G. Xie, Z. Liu, Z. Zhu, Q. Liu, J. Ge, and Z. Huang, *Journal of Catalysis*, 2004, **224**(1), 42–49.